Phanerozoic tectonothermal events of the Xuefengshan Belt, central South China: Implications from Usingle bondPb age and Lusingle bondHf determinations of granites

Yang Chu, Wei Lin, Michel Faure, Qingchen Wang, Wenbin Ji

▶ **To cite this version:**

Yang Chu, Wei Lin, Michel Faure, Qingchen Wang, Wenbin Ji. Phanerozoic tectonothermal events of the Xuefengshan Belt, central South China: Implications from Usingle bondPb age and Lusingle bondHf determinations of granites. Lithos, 2012, 150, pp.243-255. ⟨10.1016/j.lithos.2012.04.005⟩. ⟨insu-00723076⟩

HAL Id: insu-00723076

https://insu.hal.science/insu-00723076v1

Submitted on 9 Aug 2012

HAL is a multi-disciplinary open access archive for the deposit and dissemination of scientific research documents, whether they are published or not. The documents may come from teaching and research institutions in France or abroad, or from public or private research centers.

L'archive ouverte pluridisciplinaire **HAL**, est destinée au dépôt et à la diffusion de documents scientifiques de niveau recherche, publiés ou non, émanant des établissements d'enseignement et de recherche français ou étrangers, des laboratoires publics ou privés.

HAL Authorization

Phanerozoic tectonothermal events of the Xuefengshan Belt, central South China: Implications from U—Pb age and Lu—Hf determinations of granites

- Yang Chu[ab] [c]
- Wei Lin[a]
- Michel Faure[ab]
- Qingchen Wan[a]
- Wenbin Ji[ac]

- [a] State Key Laboratory of Lithopheric Evolution, Institute of Geology and Geophysics, Chinese Academy of Sciences, Beijing 100029, PR China
- [b] Institut des Sciences de la Terre d'Orléans, Campus Géosciences, Université d'Orléans, 1A, Rue de la Férollerie, 45071 Orléans Cedex 2, France
- [c] Graduate University of Chinese Academy of Sciences, Beijing 100049, PR China

Abstract

The Xuefengshan Belt, characterized by large-scale fold and thrust structures and widespread granites, is a key area to decipher the tectonic evolution of the South China block. In this belt, two magmatic episodes are recorded by Early Paleozoic and Early Mesozoic granites. In this paper, we carried out precise SIMS zircon U—Pb dating and *in situ* Lu—Hf isotopes measurements on these granitic plutons. Our study indicates that the Early Paleozoic and the Early Mesozoic granites are late-orogenic products of the Early Paleozoic orogen and the Middle Triassic Xuefengshan orogen, respectively. In the Xuefengshan Belt, the Early Paleozoic event is poorly registered, since this area corresponds to the outer zone of the early Paleozoic orogen. The Silurian–Early Devonian granites are late-orogenic plutons emplaced after the main tectonic and metamorphic stage in the Wuyi–Baiyun–Yunkai belt, coeval with a widespread, subsequent extensional event in eastern and southern South China. On the other hand, Triassic granites are formed in an intracontinental environment with weakly to strongly peraluminous signatures. Zircon U—Pb ages presented here, associated with a summary of newly acquired data in the same region, suggest that the emplacement of anatectic granites occurred around 225–215 Ma, not in a rather wide range of ca. 245–200 Ma. *In situ* zircon $\varepsilon_{Hf}(t)$ values indicate a crust-derived source without a mantle-derived input for the two generations of granites. Combining our data with recent studies, we infer that the central area of the South China block has experienced two tectonothermal events: the Early Paleozoic magmatism developed as a result of the collapse of the Early Paleozoic orogen, while these Early Mesozoic granites can be the late-orogenic products of the intracontinental Xuefengshan orogen, most likely manifesting the far field effect by the subduction of the Paleo-Pacific ocean plate at the southeastern margin of the South China block.

Highlights

► Precise SIMS zircon U—Pb ages are presented from the Xuefengshan Belt. ► Early Paleozoic late-orogenic magmatism was widespread in the South China block. ► The Middle Triassic Xuefengshan orogeny ended with late-orogenic granites. ► The Triassic magmatism of this belt is precisely constrained during 225–215 Ma.

Keywords

Phanerozoic tectonothermal events; Xuefengshan Belt; SIMS U—Pb zircon dating; Lu—Hf isotopes; South China

1. Introduction

Accompanied with remarkable shortening and thickening of continental crust, crustal melting is a common phenomenon in many orogenic belts, such as Himalaya, Qinling–Dabie, and Variscan belts ([Brown, 2005], [Chung et al., 2005], [Faure et al., 2003], [Faure et al., 2008] and [Harris and Massey, 1994]). This feature represents the thermal relaxation during late-, or post-collisional removal or unthickening process of the uplifted mountain belts.

In South China, granitic plutons provide a window to investigate the tectonic evolution of this large piece of continental crust. It has been well accepted that several tectonothermal events occurred in Early Paleozoic, Early Mesozoic and Late Mesozoic ([Chen, 1999], [Faure et al., 2009], [Li and Li, 2007], [Li et al., 2010b], [Wang et al., 2005], [Yan et al., 2003], [Zhou and Li, 2000] and [Zhou et al., 2006]). Contemporaneous with considerable granitic intrusions, coeval volcanism and regional normal and strike-slip faulting, the Yanshannian event is systematically studied by multidisciplinary approaches, and interpreted as an extensional tectonics in response to the SE-directed subduction of the Pacific Plate ([Faure et al., 1996], [Lin et al., 2000], [Shu et al., 2009] and [Zhou et al., 2006]). However, the Early Paleozoic and the Early Mesozoic events remain poorly understood in spite of their recognition several decades ago ([Huang, 1960] and [Huang, 1978]). Recent studies suggest that the Early Paleozoic and Early Mesozoic orogens are both intracontinental ([Charvet et al., 2010], [Chu et al., 2011], [Chu et al., in press], [Faure et al., 2009], [Li et al., 2010b] and [Wang et al., 2005]). The Early Paleozoic orogenic belt in South China (Fig. 1), demonstrated by a regional Devonian unconformity, Silurian–Early Devonian magmatism and high-grade metamorphism, is located in the southeastern part of the South China block from the Wuyi in the northeast, the Baiyun in the middle, to the Yunkai in the southwest ([Li et al., 2010b], [Li et al., 2011], [Wan et al., 2010], [Wang et al., 2007b] and [Yang et al., 2010]). Now it is accepted that the Early Paleozoic belt was an intracontinental orogen that developed in response to the closure of the Nanhua rift ([Charvet et al., 2010], [Faure et al., 2009] and [Li et al., 2010b]).

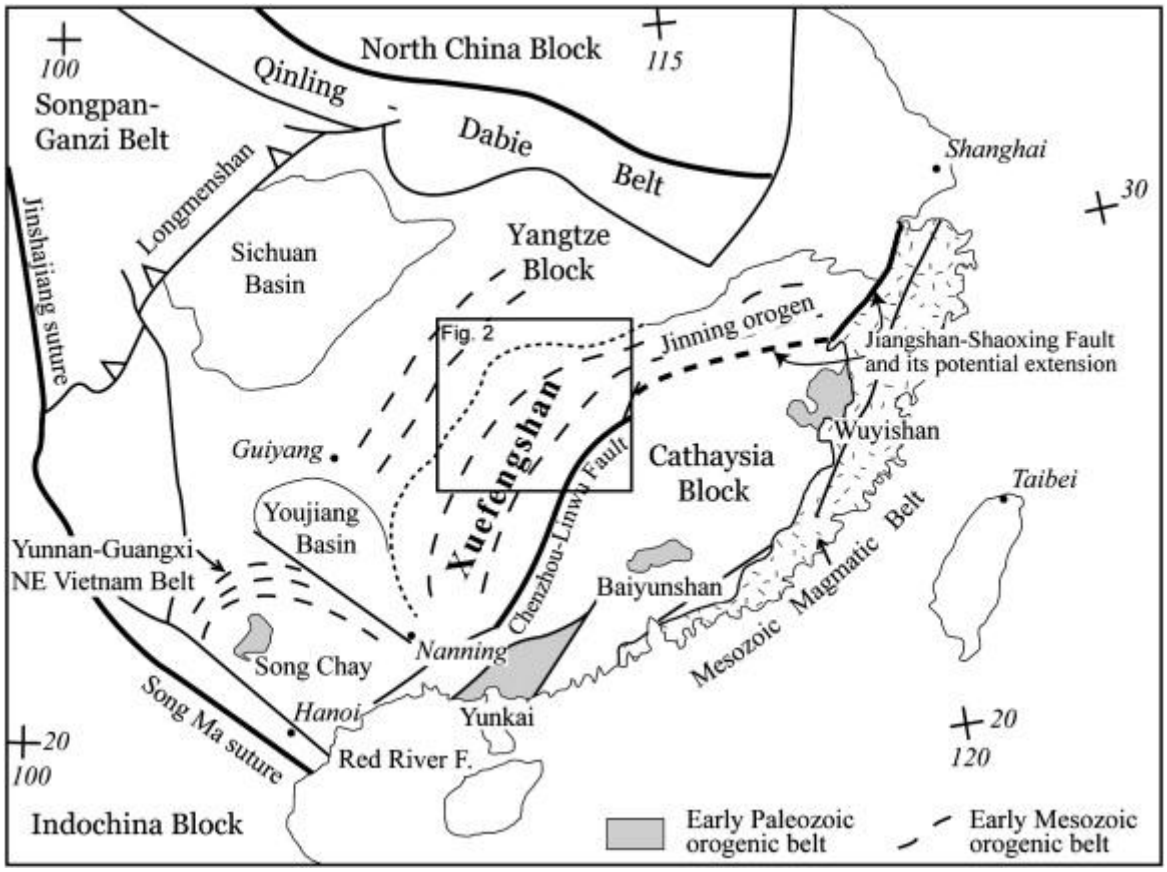

Fig. 1. Tectonic framework of the South China block.

Except the Sichuan Basin, the entire South China block was involved in the Early Mesozoic event (Fig. 1), where Early Paleozoic structures underwent intensive overprinting. In the central part of the South China block, the Xuefengshan Belt was identified by detailed structural analysis as a Triassic intracontinental orogen ([Chu et al., 2011] and [Chu et al., in press]). Previous studies suggested that Early Mesozoic igneous rocks are widespread in the South China block, especially in Hunan province, as syn- or late-orogenic products. However, the timing of the magmatism, lasting from 245 Ma to 200 Ma, is still in variance. Furthermore, the petrogenesis and geodynamic background of the Triassic plutons are also in debate ([BGMRHN, 1988], [Chen et al., 2006], [Chen et al., 2007a], [Chen et al., 2007b], [Ding et al., 2005], [Li and Li, 2007], [Li et al., 2008], [Wang et al., 2007a], [Xu et al., 2004] and [Xu et al., 2005] and reference therein).

In this work, we report SIMS U—Pb zircon ages and *in situ* Lu—Hf isotopic data from the Early Paleozoic and Early Mesozoic granites that crop out in the Xuefengshan Belt, in Hunan Province, in order to precisely constrain the timing of magmatic activities. We demonstrate that the Early Mesozoic granitic plutons represent orogenic products related to the Xuefengshan Belt, whereas, the Early Paleozoic ones emplaced in the late orogenic stage of the Early Paleozoic orogeny, and experienced an important post-solidus reworking during the Early Mesozoic tectonics. A possible interpretation of their potential source, and tectonic implications of the two tectonothermal events with respect to the South China block are also discussed.

2. Geological setting

From Neoproterozoic to Cenozoic, over 10-km-thick sedimentary rocks cover most of the South China block. Nevertheless, crustal information on almost unexposed Archean to Paleoproterozoic crust is provided by locally distributed basement rocks and chronological data of detrital zircons in the Yangtze block and the Cathaysia block ([BGMRFJ, 1985], [BGMRHN, 1988], [BGMRZJ, 1989], [Qiu et al., 2000], [Yu et al., 2009], [Yu et al., 2010], [Zhang et al., 2006a], [Zhang et al., 2006b], [Zheng et al., 2004] and [Zheng et al., 2010]).

During the Neoproterozoic, the South China Block was finally amalgamated by collision between the Yangtze and the Cathaysia blocks, separated by the Jinning (or Sibao) orogen (Fig. 1, cf. Li et al., 2009a), which has been documented by structural, geochemical and geochronological data ([Charvet et al., 1996], [Li, 1999], [Li et al., 2002], [Li et al., 2009a] and [Shu et al., 1994], and references therein). Since the Neoproterozoic, the South China Block experienced a relatively quiet period of ~ 400 Ma until the Early Paleozoic intracontinental tectonics, or named as the Wuyi–Yunkai orogen, which is responsible for ductile shearing, Devonian regional unconformity, high-grade metamorphism, and crustal melting ([BGMRJX, 1984], [Charvet et al., 2010], [Faure et al., 2009], [Huang, 1960], [Li et al., 2010b], [Ren, 1991] and [Wan et al., 2010]). At the end of this orogeny, widespread Silurian-Devonian plutons intruded into pre-Devonian syntectonic metamorphic rocks. In the Xuefengshan area (Fig. 2), in spite of several granites, the Early Paleozoic event is not as pervasive as in the Wuyi–Baiyun–Yunkai area, as its distance from the core area involved in the Wuyi–Yunkai orogen is more than 500 km. Conversely, the NE–SW trending structures are related to the Early Mesozoic event, which is called the Xuefengshan orogeny. This Middle Triassic orogeny is revealed by a regional unconformity between the Late Triassic-Early Jurassic terrigenous rocks and pre-Middle Triassic deformed rocks ([BGMRGX, 1985], [BGMRHN, 1988] and [Shu et al., 2009]).

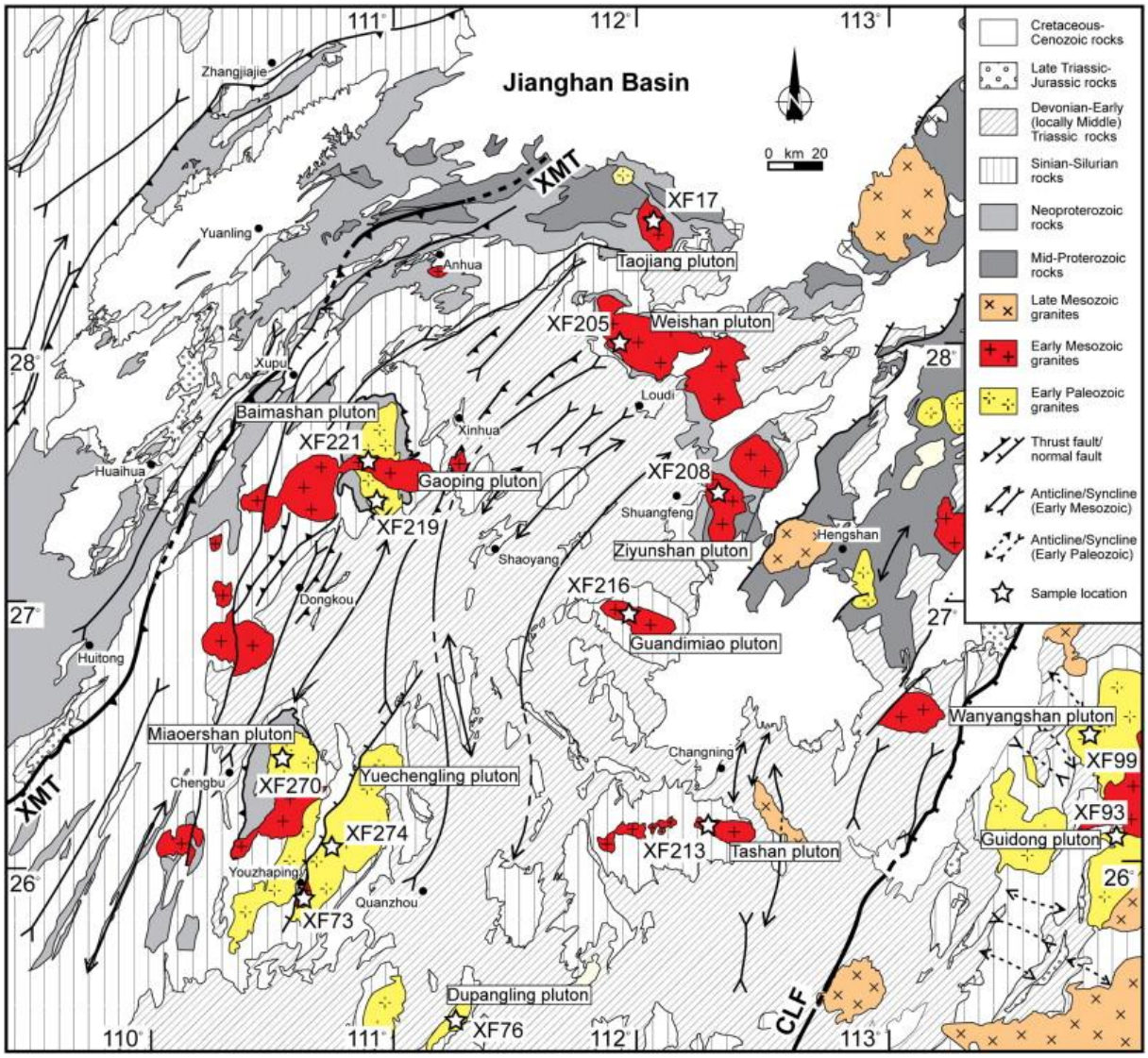

Fig. 2. Geologic map of the Xuefengshan Belt with sample locations of granites XMT: The Xuefengshan Main Thrust. CLF: The Chenzhou-Linwu Fault.

The Early Mesozoic event in South China is often called the Indosinian Orogeny, but in fact this name was originally used to account for the Triassic tectonic event by unconformities between pre-Norian and pre-Rhaetian in Vietnam ([Deprat, 1914] and [Fromaget, 1932]). The South China block also experienced Triassic event contemporary to the "Indosinian orogeny" (e.g. [Chu et al., 2011] and [Wang et al., 2005]). However, these two tectonic events are relevant of different geodynamics. Therefore, it is better to separate the tectonic event of Vietnam from the simultaneous events in South China by using different names so as to avoid confusion. In central South China, the Middle Triassic intracontinental Xuefengshan Belt is characterized by well developed thrust faults, folds and pervasive cleavages in the sedimentary cover, and ductile syn-metamorphic deformation with a NE–SW striking foliation and a NW–SE trending lineation developed in a decollement layer and basement rocks. Late Triassic granites intruded into the folded strata as late-orogenic products ([Chu et al., 2011], [Chu et al., in press], [Qiu et al., 1999] and [Wang et al., 2007a]). The region to the east of the Chenzhou–Linwu fault is dominated by WNW–ESE trending structures of Early

Paleozoic age (Fig. 2), whereas to the west, NE–SW trending, Early Mesozoic structures are the most noticeable features. Hence, the Chenzhou–Linwu fault acted as an important tectonic boundary in central South China. This fault is also postulated to be the southwest extension of the Neoproterozoic suture zone ([Wang et al., 2003] and [Wang et al., 2007b]).

3. Analytical procedures and sample description

3.1. Zircon U—Pb dating

Zircons were separated from samples using standard density and magnetic separation techniques. Zircon grains, together with standard Plešovice and Qinghu zircons were mounted in epoxy mounts that were then polished to section the crystals in half for analysis. All zircons were photographed in transmitted and reflected light, and the cathodoluminescence (CL) image in order to reveal their internal structures. The mount was vacuum-coated with high-purity gold for SIMS analyses.

The U—Pb determination was conducted using a Cameca IMS 1280 large-radius SIMS at the Institute of Geology and Geophysics, Chinese Academy of Sciences (CAS) in Beijing. U—Th—Pb ratios and absolute abundances were determined relative to the standard zircon Plešovice (Sláma et al., 2008). Analytical procedures are the same as those described by Li et al. (2009b). The ellipsoidal spot is about 20 × 30 μm in size. Positive secondary ions were extracted with a 10 kV potential. A long-term uncertainty of 1.5% (1 RSD) for $^{206}Pb/^{238}U$ measurements of the standard zircons was propagated to the unknowns (Li et al., 2010a), despite that the measured $^{206}Pb/^{238}U$ error in a specific session is generally around 1% (1 RSD) or less. Correction of common lead was made by measuring ^{204}Pb. An average Pb of present-day crustal composition (Stacey and Kramers, 1975) is used for the common Pb assuming that it is largely due to surface contamination introduced during sample preparation. Uncertainties on individual analyses in data tables are reported at a 1σ level; mean ages for pooled U/Pb (and Pb/Pb) analyses are quoted with 95% confidence interval. Data reduction was carried out using the Isoplot program (Ludwig, 2001).

3.2. Zircon Lu—Hf isotopes

Zircon Lu—Hf isotopic analysis was carried out *in situ* on a Neptune multi-collector ICP-MS equipped with a Geolas-193 laser ablation system at the Institute of Geology and Geophysics, Chinese Academy of Sciences. Detailed analytical procedures are given in Wu et al. (2006). Previously analyzed zircon grains for U-Pb isotopes were chosen for Lu—Hf isotopic analyses. The beam diameter is either 44 or 60 μm, with a laser repetition rate of 10 Hz at 100 mJ. During the analytical period, the weighted mean $^{176}Hf/^{177}Hf$ ratios of the zircon standards GJ-1 (0.281999 ± 6, 2σ, n = 34) and MUD (0.282503 ± 7, 2σ, n = 34) are in good agreement with reported values ([Morel et al., 2008] and [Woodhead and Hergt, 2005]).

3.3. Sample description

The Early Paleozoic granites are mostly distributed in the southern and eastern parts of the Xuefengshan Belt with a total area over 3000 km^2. The selected samples (XF76, XF93, XF99, XF219, XF270, and XF274) are dominantly biotite monzogranite, biotite granite and hornblende-bearing granite with intermediate to coarse-grained texture. They commonly consist of biotite (~ 10%), K-feldspar (~ 25%), plagioclase (~ 35%) and quartz (~ 30%), with a minor amount of hornblende or muscovite and other accessory minerals.

Early Mesozoic granites make up the largest portion, over 5000 km^2 in area (BGMRHN, 1988). Similar to Early Paleozoic granites, these Triassic granites (XF17, XF73, XF205, XF208, XF213, XF216 and XF221) are biotite monzogranite and biotite granite, whereas two types are distinguished on the basis of the presence of hornblende or muscovite (Fig. 3a–b). The mineral assemblage is biotite (~ 8%), plagioclase (~ 40%), K-feldspar (~ 20%), and quartz (30%), with minor hornblende (~ 2%) or muscovite (~ 2%). A good consistence of granite type is also shown by that the A/CNK index of the hornblende bearing granites (XF17, XF216 and XF221) ranges 1.0 to 1.1 as an aluminous type, whereas the index of the muscovite-bearing granites (XF73, XF205, XF208 and XF213) is higher than 1.1, indicating a peraluminous magmatic type (Wang et al., 2007a).

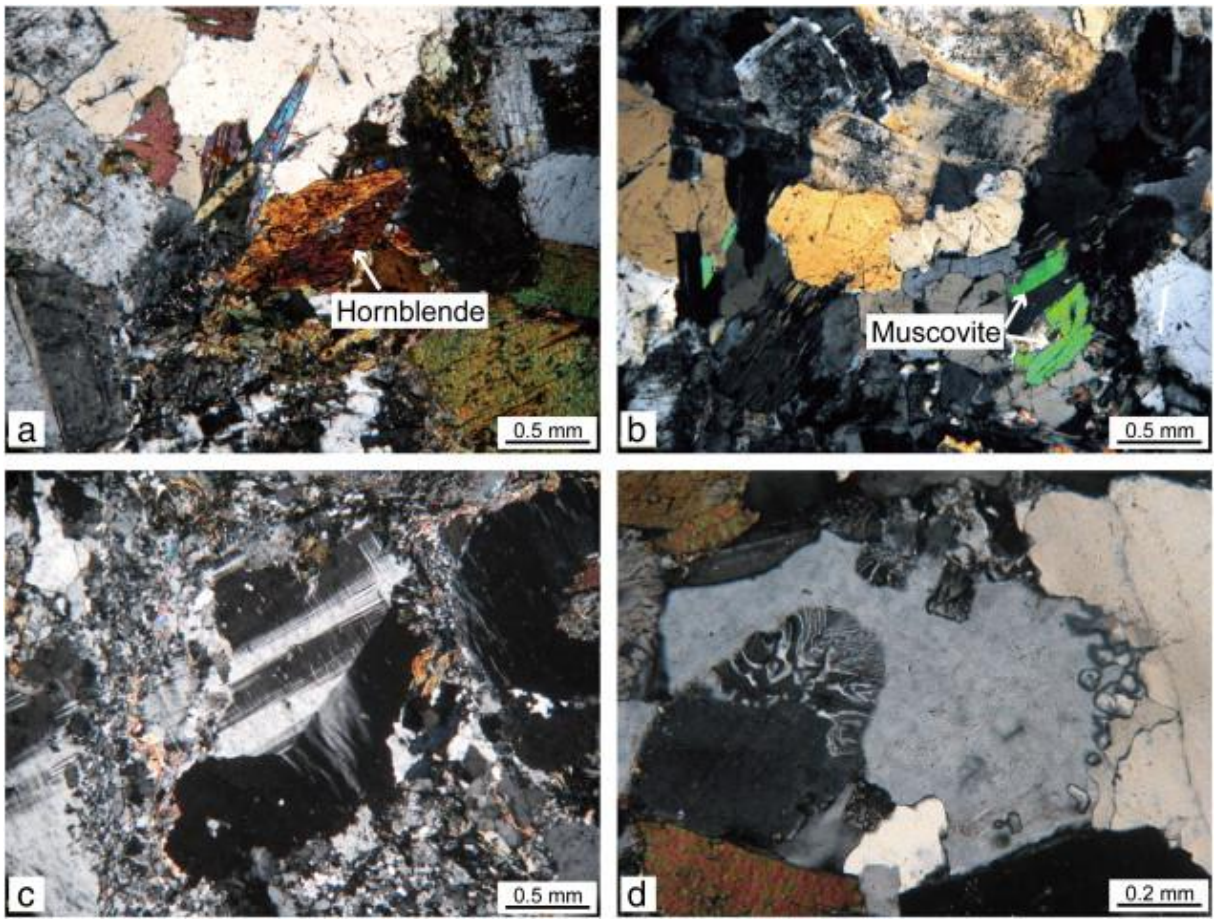

Fig. 3. Microscopic photos of granites. Two types of Triassic granites: (a): Hornblende-bearing granite. (b): Muscovite-bearing granite. Different deformation patterns in (c) the Paleozoic granite with quartz dynamic recrystallization and twins in plagioclases, and (d) the Mesozoic granite with no obvious ductile deformation but mymekites as an indicator of pre-solidus deformation.

Additionally, the structures of granites of the two generations are different. Along the boundary of the Early Paleozoic granites (e.g. Baimashan pluton), rocks are sheared with a deformed zone of several hundred meters wide. In this zone, quartz grains are strongly recrystallized around plagioclase, which also show undulose or flame-shape extinction (Fig. 3c). This post-solidus fabric is due to the Early Mesozoic deformation event. In contrast, the deformation structure is rare or absent in the Early Mesozoic granites (Fig. 3d). In these

rocks, a magmatic structure with weakly deformed quartz and feldspar grains, commonly with myrmekite textures is dominant.

4. Results

Sample locations are shown in the Fig. 1. The zircon U—Pb analytical data are listed in Supplementary data Table 1, and concordia ages are presented in Fig. 5 and Fig. 6. Lu—Hf isotopic results are listed in Supplementary data Table 2, and diagrams of $\varepsilon_{Hf}(t)$ and Hf crustal model ages are shown in Fig. 7.

4.1. SIMS zircon U—Pb age

4.1.1. Early Paleozoic granites samples

Six samples were collected from Early Paleozoic granites of the Xuefengshan Belt (see detailed GPS location in Table 1).

Table 1. Summary of sample localities of Early Paleozoic and Early Mesozoic granites in the Xuefengshan Belt.

Pluton	Sample no.	Lithology	GPS	Age (Ma)	Error (Ma)	Reference
Early Mesozoic plutons						
Taojiang	XF17	Hornblende biotite granite	N28°28.624′, E112°04.268′	220	2	This study
Yuechengling–Youzhaping	XF73	Biotite granite	N25°56.121′, E110°38.082′	219	2	This study
Tashan	XF213	Biotite granite	N26°11.709′, E112°16.528′	224	2	This study
Guandimiao	XF216	Hornblend monzogranite	N26°57.392′, E112°08.094′	225	2	This study
Baimashan (Gaoping)	XF221	Hornblend granite	N27°35.756′, E110°58.355′	217	2	This study
Weishan	XF205	Biotite monzogranite	N28°00.255′, E112°00.455′	222	3	Chu et al., in press
Ziyunshan	XF208	Biotite monzogranite	N27°27.802′, E112°22.327′	225	2	Chu et al., in press
Early Paleozoic plutons						
Dupangling	XF76	Biotite monzogranite	N25°20.102′, E111°05.427′	428	4	This study
Guidong	XF93	Hornblend granite	N26°05.496′, E113°58.364′	438	3	This study
Wanyangshan	XF99	Two-mica granite	N26°27.393′, E113°49.097′	437	4	This study
Baimashan (Main)	XF219	Hornblend granite	N27°27.948′, E110°57.279′	411	4	This study
Miaoershan	XF270	Biotite granite	N26°27.690′, E110°30.608′	412	4	This study
Yuechengling (Main)	XF274	Biotite granite	N26°10.109′, E110°43.674′	424	3	This study

Sample XF76 is a monzonite from the Dupangling pluton, in the southern part of the study area. The zircon grains from this sample are subhedral with straight grain margins, and are mostly clear and colorless to light brown or pink in color in transmitted light image. The grains have aspect ratios of between 2:1 and 4:1 with long axes of 100–200 μm (Fig. 4). Sixteen spots on these zircons have relatively low U (210–564 ppm) and Th (45–283 ppm) contents, with Th/U ratios from 0.128 to 0.652, except for one grain (XF76 at 10). Excluding 3 inherited grains at 956 Ma, 823 Ma and 803 Ma, a concordia age at 428 ± 4 Ma is calculated, indicative of the granite emplacement time (Fig. 5a).

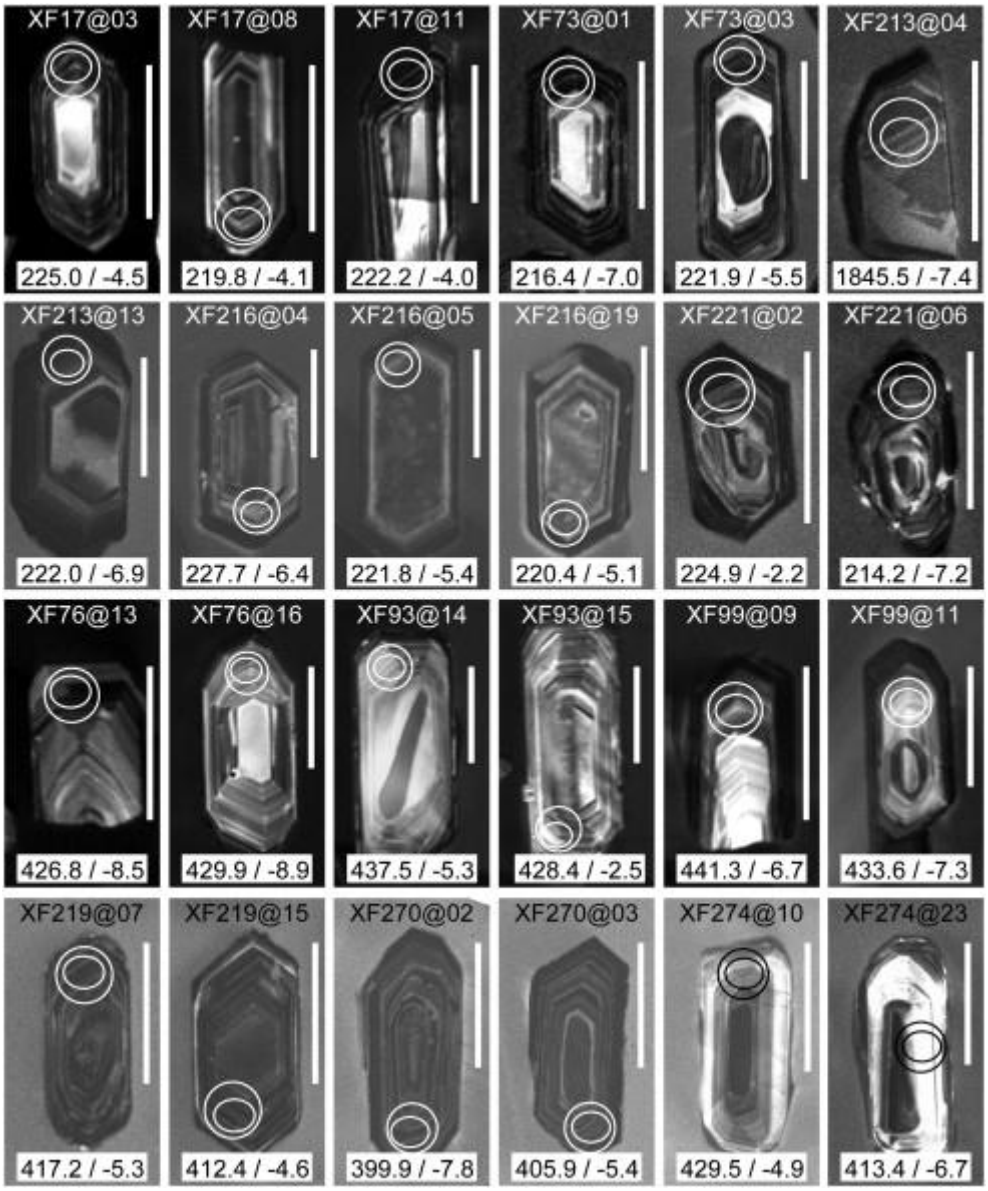

Fig. 4. Cathodoluminescence (CL) images of representative zircons from collected granite samples. Small ellipses are locations of SIMS U—Pb analysis spots and circles indicate the locations of LA-MC-ICPMS Hf analyses. Age and $\varepsilon_{Hf}(t)$ data are listed under individual zircons with ages ahead. The scale bar is 50 μm.

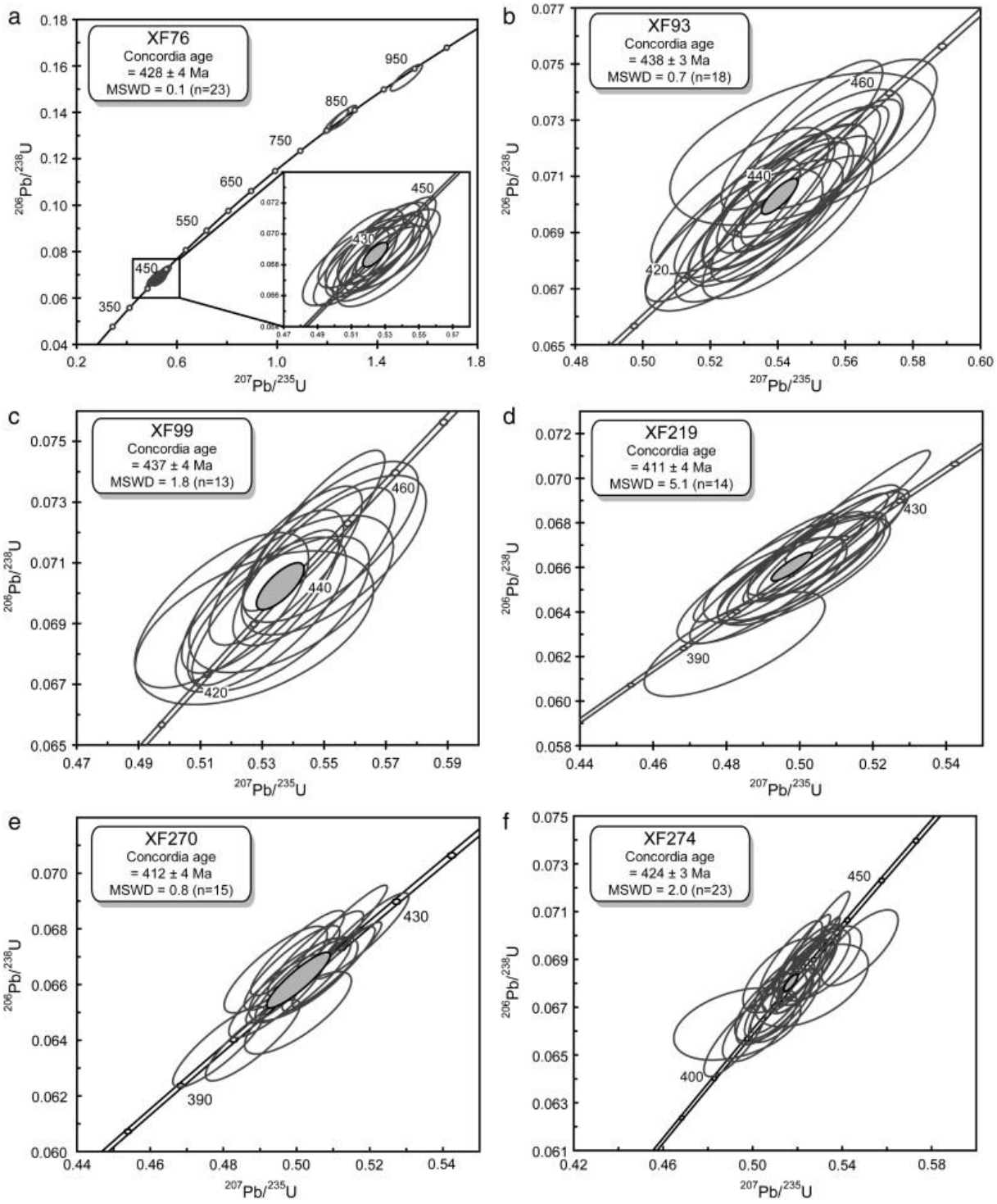

Fig. 5. SIMS U—Pb concordia diagrams of Early Paleozoic granite samples.

Sample XF93 is collected from the Guidong pluton. Zircon grains from this sample are euhedral, transparent, and 50–300 μm in length with aspect ratios between 2:1 and 3:1. They are characterized by fine, euhedral concentric zoning under CL images (Fig. 4); inherited cores are occasionally visible. Eighteen analyses were performed on the magmatic rims. The U concentration ranges from 272 to 673 ppm, Th from 88 to 235 ppm, and Th/U ratios from 0.286 to 0.503. A concordia age of 438 ± 3 Ma is given, representing the crystallization time of the pluton (Fig. 5b).

Sample XF99 is from the Wanyangshan pluton. Thirteen analyses on 13 zircon grains were carried out. Most zircons from this sample are euhedral, transparent, 100–300 μm in length, and have aspect ratios of 2:1 to 3:1. Euhedral concentric zoning is common in CL images (Fig. 4). The analyzed grains present U and Th contents of 122 to 812 ppm, 49 to 297 ppm, respectively. Th/U ratios range from 0.146 to 0.907. The $^{206}Pb/^{238}U$ and $^{207}Pb/^{235}U$ results plotted on a concordia diagram show a consistent group distribution, yielding a concordia age of 437 ± 4 Ma corresponding to the crystallization age of the pluton (Fig. 5c).

Sample XF219 is collected from the Baimashan pluton. Zircon grains are euhedral, transparent and 150–300 μm long with aspect ratios between 2:1 and 4:1. Concentric zoning is common in CL images. Zircons from sample XF219 yield the U concentrations from 318 to 2086 ppm, Th from 191 to 1271 ppm, and Th/U ratios from 0.327 to 0.910. Fourteen analyses of the $^{206}Pb/^{238}U$ and $^{207}Pb/^{235}U$ results plotted on a concordia diagram show a consistency group distribution with a concordia age of 411 ± 4 Ma, interpreted as the crystallization age (Fig. 5d).

Sample XF270 is collected from the Miaoershan pluton. Zircon grains from this sample are euhedral, transparent, and 50–300 μm in length with aspect ratios between 2:1 and 3:1. Euhedral concentric zoning is well displayed in CL images (Fig. 4). Fourteen analyses of 14 zircons were obtained, with moderate U (480–1827 ppm) and Th (160–1223 ppm) concentrations. The Th/U ratios vary from 0.288 to 0.692. All analyses yield a concordia age of 412 ± 4 Ma (Fig. 5e), which is interpreted as the granite crystallization age.

Sample XF274 is collected from the Yuechengling pluton, which is ductilely deformed along its margin. The zircons extracted from the sample show euhedral to subhedral grain shapes with straight grain boundaries. They have aspect ratios from 1:1 to 3:1. Grain long axes are 150–200 μm (Fig. 4). These zircon grains show oscillatory zoning in the CL image. Twenty-three analyses of 23 zircons were obtained. The contents in U and Th, and Th/U ratios vary from 116 to 2453, 139 to 951 and 0.230 to 1.263, respectively. The plots of analytic results are relatively consistent with one group of distribution. A concordia age of 424 ± 3 Ma is interpreted as the crystallization age of the pluton (Fig. 5f).

4.1.2. Samples of Early Mesozoic granites

Five samples were collected from Early Mesozoic plutons and dated by SIMS U—Pb methods.

Sample XF17 is a biotite granite collected from the Taojiang pluton. Zircon grains are euhedral, transparent, and 150–250 μm in length with aspect ratios between 1.5:1 and 3:1. Euhedral concentric zoning is common in most grains in CL images (Fig. 4). Thirteen analyses of 13 zircons were obtained. The concentrations of U and Th range from 238 to 1520 ppm, and from 131 to 871 ppm, respectively. Th/U ratios range from 0.277 to 0.710. All analyses have a concordia age of 220 ± 2 Ma (Fig. 6a), which is interpreted as the emplacement age of the granitic pluton.

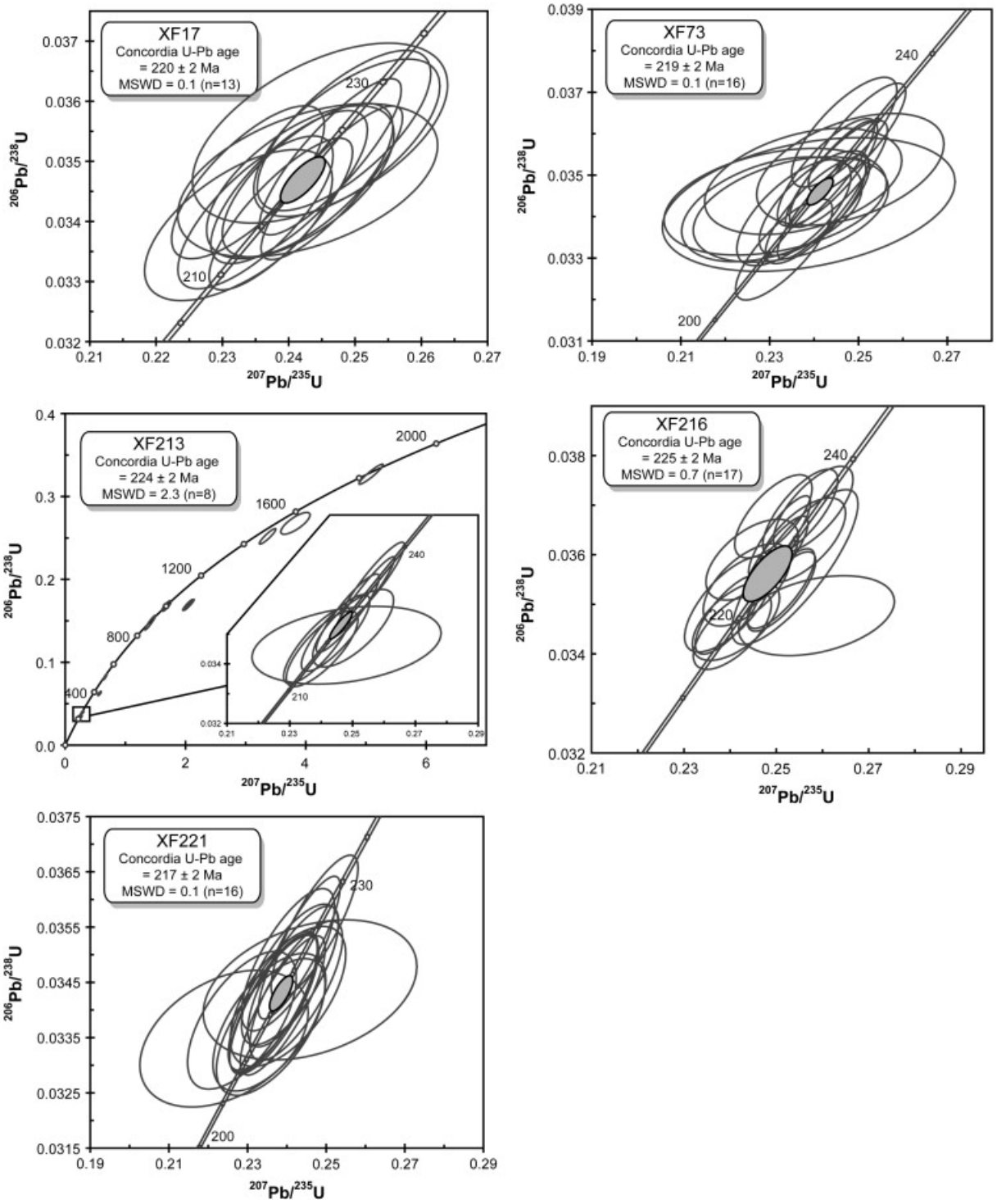

Fig. 6. SIMS U—Pb concordia diagrams of Early Mesozoic granite samples.

Sample XF73 is a monzonitic granite collected from the Yuechengling pluton. Most zircon grains from this sample are euhedral, transparent, and 150–300 μm in length with aspect ratios between 1:1 and 3:1. Euhedral concentric zoning is common in most zircon grains in CL images (Fig. 4); these images show that inherited zircon cores have magmatic overgrowths within a few grains. Sixteen analyses of 16 zircons were obtained. These zircons have intermediate U (162–2486 ppm) and Th (154–1416 ppm) contents, with Th/U ratios

from 0.221 to 1.575. A concordia age of 219 ± 2 Ma is obtained (Fig. 6b), representing the crystallization time of the pluton.

Sample XF213 is a biotite granite collected from the Tashan pluton. Some of the zircon grains show inherited cores and variably-sized concentric zoning, whereas other grains are magmatic without inherited cores. Inherited zircons are round, transparent, and 50–150 μm in length with aspect ratios between 1:1 and 2:1; while magmatic zircons are euhedral, and 100–250 μm in length with aspect ratios between 2:1 and 3:1 (Fig. 4). Seventeen analyses of 17 zircons have variable U content of 47 to 3964 ppm, low Th content of 23 to 373 ppm; Th/U ratios range from 0.009 to 1.191. Eight out of 17 analyses yield a consistent concordia age cluster at 224 ± 4 Ma, which is taken as the crystallization age of the granite (Fig. 6c). The remaining 9 analyses, plotted along the concordia curve, give variable apparent ages ranging from 251 to 1823 Ma, including some less concordant ages at 1002 Ma, 1448 Ma and 1528 Ma. These zircons are interpreted as inherited ones from the magma source.

Sample XF216 is collected from an amphibole-bearing granite in the Guandimiao pluton. Zircon grains from this sample are euhedral, transparent, and 100–200 μm in length with aspect ratios between 2:1 and 4:1 (Fig. 4). Nineteen analyses of 19 zircons, with 280 to 4484 ppm of U, 189 to 4577 ppm of Th, and 0.386 to 1.021 of Th/U ratios, yield a concordia age of 225 ± 2 Ma, representing the crystallization age for this sample, except the zircon grain (XF216 at 9) that gives an abnormally young age (Fig. 6d).

Sample XF221 is a monzonitic granite collected in the Baimashan (Gaoping) pluton. Most zircon grains are euhedral, transparent, colorless and 150–300 μm in length with aspect ratios between 2:1 and 4:1. Euhedral concentric zoning is common in most grains in CL images (Fig. 4); inherited zircon cores are rare. Sixteen analyses of sixteen zircons were obtained with 191 to 1559 ppm of U, 87 to 713 ppm of Th, and 0.263 to 0.746 of Th/U ratios, yielding a concordia age of 217 ± 2 Ma (Fig. 6e). This age is considered as the emplacement age of this pluton.

4.2. Zircon Lu—Hf isotopes

Most of the Lu—Hf isotope analyses were performed on spots within the same internal structure domains that were analyzed for U/Pb isotopic compositions. In addition to the abovementioned samples, samples XF205 from the Weishan pluton, and XF208 from the Ziyunshan pluton (Table 1) were also analyzed for the Lu—Hf composition. The concordia ages of the plutons obtained from zircons of the same sample were used for calculating their initial Hf isotopic ratios and the crustal model ages. 113 analyses were performed on 6 samples from Early Paleozoic granites, and 148 analyses were performed on 7 samples from Early Mesozoic granites, including XF205 and XF208, which were dated by Chu et al. (submitted for publication). These results are presented in Supplementary data Table 2. Diagrams of $\varepsilon_{Hf}(t)$ values are shown in Fig. 7.

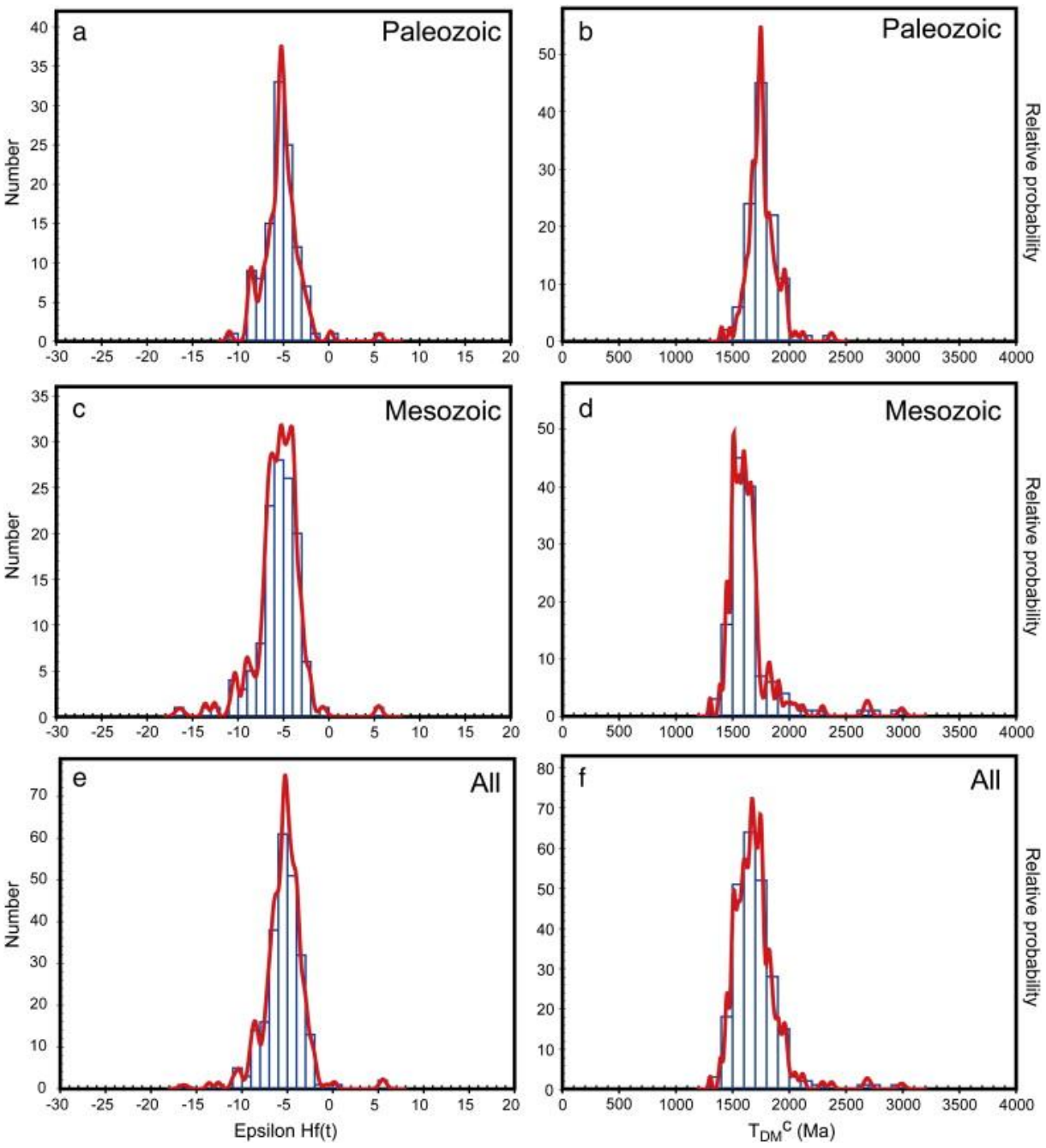

Fig. 7. Diagrams of $\varepsilon_{Hf}(t)$ and T_{DM}^{C} values from Early Paleozoic granites (a–b), Early Mesozoic granites (c–d) and all samples (e–f) in the Xuefengshan Belt.

4.2.1. Samples from Early Paleozoic granites

Seventeen zircons were chosen from sample XF76 to perform Hf analyses. The zircon grains with Early Paleozoic ages have invariable Hf isotopic compositions with $^{176}Hf/^{177}Hf$ ratios ranging from 0.282269 to 0.282313. The calculated $\varepsilon_{Hf}(t)$ values range from − 8.9 to − 6.1, and their T_{DM}^{C} ages vary from 1807 to 1979 Ma. Additionally, in three inherited zircon grains, a positive $\varepsilon_{Hf}(t)$ value (+ 5.6) is obtained with a T_{DM}^{C} age at 1475 Ma. The other two grains give $\varepsilon_{Hf}(t)$ values of − 3.0 and − 5.4, and T_{DM}^{C} ages of 1914 Ma and 2050 Ma, respectively.

In sample XF93, twenty-two analyses of 22 zircons show variable Hf isotopic compositions with $^{176}Hf/^{177}Hf$ ratios ranging from 0.282294 to 0.282440. The calculated $\varepsilon_{Hf}(t)$ values range from − 7.5 to − 2.5, and their T_{DM}^{C} ages are between 1583 Ma and 1903 Ma.

In sample XF99, seventeen zircons were chosen to perform Hf analyses. Hf isotopic compositions with $^{176}Hf/^{177}Hf$ ratios vary from 0.282199 to 0.282456. The calculated $\varepsilon_{Hf}(t)$ values range from − 11.0 to − 2.2, and their T_{DM}^{C} ages vary from 1720 to 2118 Ma. One inherited zircon of 939 Ma has a $\varepsilon_{Hf}(t)$ value of − 8.8 and a T_{DM}^{C} age of 2372 Ma.

In sample XF219, eighteen zircons were chosen to perform Hf analyses, with $^{176}Hf/^{177}Hf$ ratios from 0.282329 to 0.282450, calculated $\varepsilon_{Hf}(t)$ values from − 7.0 to − 2.9, and their T_{DM}^{C} ages from 1590 Ma to 1846 Ma.

In sample XF270, nineteen analyses of 19 zircon grains were obtained. $^{176}Hf/^{177}Hf$ ratios vary from 0.282306 to 0.282463. The calculated $\varepsilon_{Hf}(t)$ values range from − 7.8 to − 2.2, and their T_{DM}^{C} ages vary from 1546 Ma to 1900 Ma.

In sample XF274, a total of twenty zircons were chosen to perform Hf analyses. $^{176}Hf/^{177}Hf$ ratios vary from 0.282325 to 0.282522. The calculated $\varepsilon_{Hf}(t)$ values vary from − 6.7 to − 1.8, with their T_{DM}^{C} ages from 1531 to 1843 Ma. Only one slightly positive $\varepsilon_{Hf}(t)$ value of + 0.2 is obtained, with a T_{DM}^{C} age at 1407 Ma.

4.2.2. Samples from Early Mesozoic granites

For sample XF17 of the Taojiang pluton, inherited cores of zircons were not analyzed. Eighteen zircons were analyzed for the Hf isotopes, yielding relatively similar $^{176}Hf/^{177}Hf$ ratios from 0.282504 to 0.282583, and $\varepsilon_{Hf}(t)$ values from − 5.0 to − 2.1. Their T_{DM}^{C} ages range from 1386 Ma to 1572 Ma.

In sample XF73, nineteen zircon grains were chosen from the Yuchengling (Youzhaping) pluton to perform Hf analyses. $^{176}Hf/^{177}Hf$ ratios vary from 0.282325 to 0.282522. The calculated $\varepsilon_{Hf}(t)$ values range from − 10.4 to − 3.1, and their T_{DM}^{C} ages vary from 1451 Ma to 1912 Ma.

In sample XF205, eighteen zircon grains were analyzed. $^{176}Hf/^{177}Hf$ ratios, from 0.282457 to 0.282556, are relatively homogeneous. Their $\varepsilon_{Hf}(t)$ values are mainly negative from − 6.6 to − 3.1. These zircons show T_{DM}^{C} ages from 1452 Ma to 1674 Ma.

In sample XF208, a total of 17 analyses on seventeen zircon grains give a $^{176}Hf/^{177}Hf$ range from 0.282457 to 0.282556. The $\varepsilon_{Hf}(t)$ values vary from − 6.3 to − 2.6, and the T_{DM}^{C} ages of these zircons range from 1427 to 1662 Ma.

Sample XF213 from the Tashan pluton has a large proportion of inherited zircons. In these inherited grains, $^{176}Hf/^{177}Hf$ ratios vary from 0.281425 to 0.282365, the $\varepsilon_{Hf}(t)$ value ranges from − 10.8 to − 2.2, with one positive value of + 5.5. The calculated T_{DM}^{C} ages vary from 1444 Ma to 2991 Ma. The analyses of the Triassic magmatic zircons show a wide range of $^{176}Hf/^{177}Hf$ ratios and $\varepsilon_{Hf}(t)$ values, which are from 0.282176 to 0.282630, and from − 16.4 to − 0.7, respectively. This type of zircons yields T_{DM}^{C} ages from 1302 Ma to 2292 Ma.

Twenty-two zircon grains from the sample XF216 of the Guandimiao pluton were analyzed and give $^{176}Hf/^{177}Hf$ ratios from 0.282437 to 0.282584, and $\varepsilon_{Hf}(t)$ values from − 7.3 to − 2.2. These zircon grains show a relatively narrow range of T_{DM}^{C} ages between 1395 and 1718 Ma.

In sample XF221, twenty analyses on zircons from the Baimashan pluton were analyzed with $^{176}Hf/^{177}Hf$ ratios from 0.282398 to 0.282525 and $\varepsilon_{Hf}(t)$ values from − 8.7 to − 4.1. The T_{DM}^{C} ages of these zircons vary from 1516 Ma to 1801 Ma.

5. Discussion

5.1. Potential source of the granitic magma

According to the geochemical characteristics, the Early Paleozoic and Early Mesozoic granites in the Xuefengshan Belt are metaluminous or peraluminous late-orogenic products ([Chen et al., 2007a], [Chen et al., 2007b], [Li, 1991], [Li, 1994], [Wang et al., 2007a], [Zhang et al., 2011], [Zhou and Li, 2000] and [Zhou et al., 2006]). Moreover, several inherited zircons also provide useful information suggesting that the potential source may be sedimentary rocks from the lower or middle crust.

The zircon $\varepsilon_{Hf}(t)$ values of the Early Paleozoic granite samples show a relatively concentrated distribution from − 10 to − 1, with a peak at − 5 (Fig. 7a). Hf crustal model ages (T_{DM}^{C}) of all the analyzed zircons range from 2.4 to 1.5 Ga, with a peak at ~ 1.75 Ga (Fig. 7b), implying a uniform parental magma source. In combination with the $\varepsilon_{Hf}(t)$ values and the Hf model ages, a homogenous lower crust with Early Mesoproterozoic and Paleoproterozoic crustal materials is preferred as the source area for Early Paleozoic granites. This result is consistent with whole rock Nd model age of the Guidong pluton (Li, 1994).

The Early Mesozoic granite samples yield a pattern of zircon $\varepsilon_{Hf}(t)$ values similar to that of the Early Paleozoic plutons (from − 10 to − 1), with a peak at around − 5 (Fig. 7c). However, the Hf crustal model ages of the Early Mesozoic granites vary from 2.3 Ga to 1.4 Ga, and the peak age (~ 1.55 Ga) is younger than that of the Early Paleozoic granites (Fig. 7d). Hence, we interpret that the Early Mesozoic granites are produced by the partial melting of Late Paleoproterozoic and Early Mesoproterozoic crustal materials. Previously reported whole rock Sm—Nd isotopic data of Early Mesozoic granites in the Xuefengshan Belt also exhibit a narrow $\varepsilon_{Nd}(t)$ range from − 11 to − 6, and likewise Nd crustal model ages around 1.5 Ga (Wang et al., 2007a). In addition, inherited zircons of ~ 1.8 Ga, ~ 1.6 Ga and 1.0 to 0.9 Ga are found in some samples, probably indicating that a Proterozoic crust survived from the partial melting. It is noteworthy that two zircons with positive $\varepsilon_{Hf}(t)$ values are found in the samples XF213 and XF76, dated at 909 Ma and 956 Ma, respectively. These values are indicative of a crustal extraction from the depleted mantle during the Neoproterozoic (Fig. 8). Because zircons with positive $\varepsilon_{Hf}(t)$ values are absent in this group of Triassic age, we consider that the Early Mesozoic magmatism was not influenced by a mantle-derived addition, but only formed at the expense of lower crustal materials.

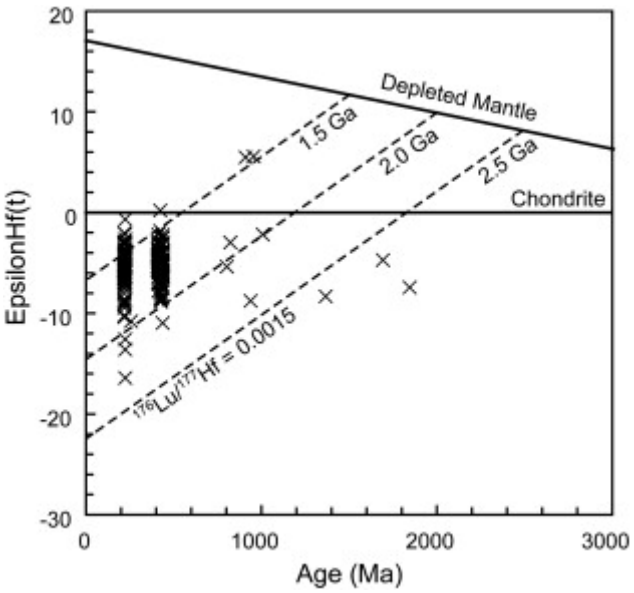

Fig. 8. Diagram of $\varepsilon_{Hf}(t)$ vs. U—Pb ages of all of zircons from Early Paleozoic and Early Mesozoic granite samples.

In summary, the two generations of Phanerozoic granitoids in the Xuefengshan Belt, Early Paleozoic and Early Mesozoic, show similar features of zircon Lu—Hf isotopes. Both generations have close $\varepsilon_{Hf}(t)$ values ranging from − 10 to − 1, with a peak at − 5 (Fig. 7e). In spite of a small time difference between the two groups of T_{DM}^{C} ages (Fig. 7f), Late Paleoproterozoic to Early Mesoproterozoic crustal materials appear to be the dominant source of the two generations of granites. In adjacent areas, Gilder et al. (1996) reported that Neodymium depleted mantle model ages range from 1.8 Ga to 1.4 Ga in Hunan and Guangxi provinces, and ~ 1.6 Ga in eastern regions. In detrital zircon records, the growth of juvenile crust also occurred between 1.7 Ga and 1.3 Ga in the Nanling-Yunkai region (Yu et al., 2010). Thus, it is concluded that these granitic magmas were mainly derived from the lower crust without addition of depleted mantle source related to the subduction.

5.2. The Early Paleozoic magmatism and its tectonic significance

An Early Paleozoic orogen extended over 2000 km in length and 600 km in width in the southeastern region of the South China block. Amphibolite-facies, or even granulite-facies metamorphism is documented in the Wuyi and Yunkai areas, during the ca. 460–440 Ma interval ([Faure et al., 2009], [Li et al., 2010b], [Wan et al., 2010] and [Wang et al., 2007b]). Moreover, late-orogenic granitoids are widespread in this orogen. Previous U—Pb results show that this magmatism probably started at ~ 450 Ma and ended at ~ 410 Ma. Our data provide a further timing constraint on granitoid emplacement in the western extension of this orogen. These ages are consistent with the zircon ages obtained by [Li, 1991] and [Li, 1994]. Compared with the Wuyi–Yunkai area, in the Xuefengshan Belt, the impact of the Early Paleozoic orogeny is limited. An Early Paleozoic ductile deformation is nearly absent in this region. Another important clue is revealed by the unconformity angle between the Middle to Late Devonian conglomerate or sandstone and pre-Devonian rocks decreases from SE to NW, and only a disconformity appears to the northwest ([BGMRHN, 1988] and [Chu et al., 2011]).

Moreover, in the central part of the Early Paleozoic orogen, the climax of syn-orogenic or late-orogenic plutonism ranges from 450 Ma to 420 Ma ([Charvet et al., 2010], [Faure et al., 2009], [Li et al., 2010b], [Wan et al., 2010], [Wang et al., 2007b], [Xu et al., 2011] and [Yang et al., 2010] and reference therein). For example, in the Wuyishan and Chencai complex, the migmatites and granites are dated at ~ 450 Ma and ~ 430 Ma, respectively (Li et al., 2010b); while in the Baiyunshan and the Yunkaidashan, the granites were emplaced from 446 Ma to 430 Ma ([Wang et al., 2007b] and [Yang et al., 2010]). However, in the Xuefengshan Belt, to the west of the Chenzhou-Linwu fault, our data indicated that the granites were emplaced ranging from 430 Ma to 410 Ma, exhibiting a time interval of 20 to 10 Ma younger in comparison with the eastern area. This difference could be resulted from that the Xuefengshan Belt represents only the outer part of the Early Paleozoic orogen, where crustal melting and ductile deformation are subsequently and weakly developed. In contrast, the major portion of the Xuefengshan Belt is dominated by the Early Mesozoic event ([Chu et al., 2011], [Chu et al., in press] and [Wang et al., 2005]). During the Early Paleozoic orogeny, around 460–440 Ma, the Wuyi–Baiyun–Yunkai region experienced crustal thickening characterized by high-grade metamorphism and ductile deformation ([BGMRFJ, 1985], [BGMRGD, 1988], [Charvet et al., 2010] and [Li et al., 2010b]). However, the Xuefengshan Belt is weakly affected by deep seated tectono-metamorphic events of Early Paleozoic age ([BGMRHN, 1988] and [Chu et al., 2011]). After the main tectono-metamorphic phase, widespread magmatism occurred in the eastern and southern regions of the belt. Peraluminous granitoids with ductile extensional structures have been interpreted as an evidence for a late-orogenic collapse ([Faure et al., 2009], [Li et al., 2010b] and [Lin et al., 2008]).

Although numerous geochronological data have been published, the geodynamics of this Early Paleozoic orogen is still debated. It is well acknowledged that a subsequent rifting, called the Nanhua rift, was developed after the Neoproterozoic collision of the Yangtze and Cathaysia blocks along the Jinning (or Sibao) orogen ([Li, 1998], [Li et al., 2009a] and [Wang and Li, 2003]). However, this rift remained in a failed state without complete breaking the South China block. Nevertheless, this event was responsible for a potential crustal weak zone along which the Early Paleozoic deformation was localized. Based on the interpretation of this failed rift, several models have been proposed to explain the inland tectonics of the South China block. According to studies on metamorphic rocks in the Yunkai region, Wang et al. (2007b) proposed an Early Paleozoic intracontinental orogen developed in response to the subduction of the Paleo-Qinling ocean the beneath the Yangtze block. However, Yan et al. (2006) interpreted the igneous activity in the Dulong-Song Chay massif as a result of the collision between the Yangtze block and the Cathaysia block by the closure of the Paleo-Tethys ocean. Recently, comprehensive studies on structural geology, petrology and geochronology support the intracontinental orogenic model ([Charvet et al., 2010], [Faure et al., 2009] and [Li et al., 2010b]). In this view, the reactivation of the Neoproterozoic Nanhua failed rift accounts well for the localization of the main tectonic and metamorphic features in the Wuyi–Baiyun–Yunkai region. The Later Silurian–Early Devonian plutons are interpreted as late-orogenic products by the collapse of the orogen.

5.3. The Early Mesozoic magmatism and its tectonic significance

In the Xuefengshan Belt, previous studies give a relatively large range of crystallization ages of the granites, resulting in various interpretations ([Chen et al., 2006], [Chen et al., 2007a], [Chen et al., 2007b], [Ding et al., 2005], [Li and Li, 2007], [Li et al., 2008], [Wang et al., 2007a], [Xu et al., 2004], [Zhou, 2007] and [Zhou et al., 2006]). [Wang et al., 2005] and [Wang et al., 2007a] suggested that a two-stage evolution of the Early Mesozoic

granites on the basis of two age-groups. The first magmatic stage, that occurred between ~ 245 Ma and 228 Ma, was generated by the readjustment of the over-thickened crust after the peak metamorphism. The second stage (220–206 Ma), was likely the result of a magma underplating event. However, our precise SIMS U—Pb dating demonstrates that the Early Mesozoic magmatism of central South China occurred in a short time span, between 225 and 215 Ma, rather than from 245 to 200 Ma. Furthermore, the metamorphic rocks of the decollement layer, which is cut by these granites, yield chemical monazite ages at 243 Ma to 226 Ma (Chu et al., in press). Therefore, the previous ages at ~ 240 Ma are questionable. We argue that all the Early Mesozoic plutons emplaced in the Xuefengshan Belt represent a single magmatic event (Fig. 9). Some authors inferred that these plutons were derived from crustal materials by decompression melting during the Late Triassic, in response to the thinning of the over-thickened curst due to the collision between South China and Indochina (e.g. [Chen et al., 2006], [Chen et al., 2007a], [Chen et al., 2007b] and [Ding et al., 2005]). However, this long-distance effect, as the Indosinian suture zone in north Vietnam is located nearly 500 km south of the Xuefengshan Belt, appears unlikely. On the contrary, Triassic granites are lacking in the in-between regions from the Vietnamese Indosinian belt to the Xuefengshan Belt. Moreover, the trend of dominant structures of the Xuefengshan Belt is perpendicular to that of the Indosinian belt. It is thereby impossible to connect the two events. Li and Li (2007) synthesized the available chronological data and proposed a flat-slab subduction model to interpret the intraplate magmatism in the South China block. Nonetheless, our Hf isotopic results imply a single magma source for the Triassic granites without any input of mantle-derived materials. Thus, it is reasonable to conclude that the flat-slab subduction did not reach the asthenosphere beneath the Xuefengshan Belt.

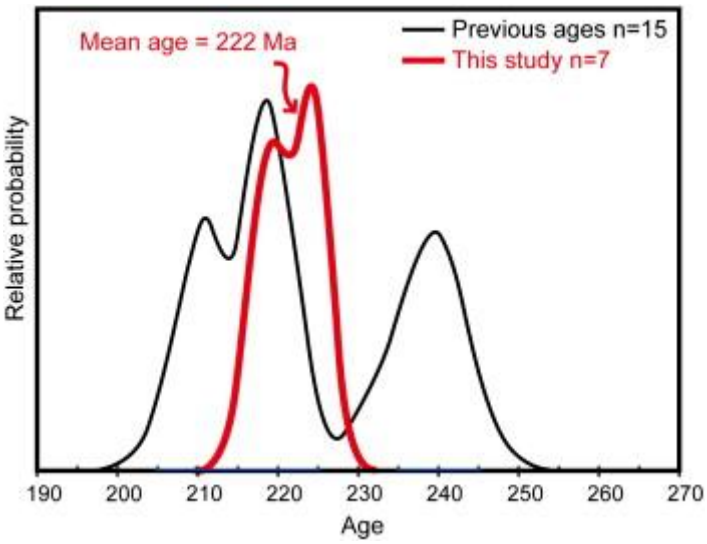

Fig. 9. Relative probability plots of isotopic ages of Triassic granites. Previous age data are from the following references ([Chen et al., 2006], [Chen et al., 2007a], [Chen et al., 2007b], [Ding et al., 2005], [Li and Li, 2007], [Li et al., 2008], [Wang et al., 2007a] and [Xu et al., 2004]).

The Xuefengshan Belt is well acknowledged as an intracontinental orogen, which was possibly triggered by the Paleo-Pacific subduction. The dominant structures are recumbent folds, thrusts, SE-dipping cleavage or foliation, and NW–SE trending lineation with top-to-the-NW shearing sense. Subsequently, a SE-vergent back-thrusting shearing and an upright folding event are well preserved (Chu et al., 2011). The orogenic stages are well constrained by our precise SIMS zircon U—Pb ages and previously obtained EMPA monazite U—Th—

Pb dating. The ductile deformation occurred in the 243–226 Ma interval, and the subsequent late-orogenic magmatism developed between 225 Ma and 215 Ma ([Chu et al., 2011] and [Chu et al., in press]).

During the Early Mesozoic, the South China block and its adjacent regions, including the western Yunnan–Indochina block, the Songpan–Gantze flysh belt, and the Qinling–Dabie-Sulu belt, experienced considerable Early Mesozoic tectonics ([BGMRGX, 1985], [BGMRJX, 1984], [Carter and Clift, 2008], [Carter et al., 2001], [Faure et al., 1999], [Hacker and Wang, 1995], [Harrowfield and Wilson, 2005], [Lepvrier et al., 1997], [Lepvrier et al., 2008], [Lepvrier et al., 2011], [Li et al., 2006], [Roger et al., 2004] and [Roger et al., 2010]), but the internal part of the block has merely raised abroad attention since recent years ([Chu et al., 2011], [Chu et al., in press] and [Wang et al., 2005]). Because of contradicting structural vergences, none of the abovementioned events can be responsible for the geodynamic setting of the Xuefengshan Belt, which was simultaneously formed during the Early Mesozoic in the center of the South China block. Thus, the introduction of a Paleo-Pacific subduction is in good coincidence with the occurrence of this intracontinental belt ([Li and Li, 2007] and [Li et al., 2006]). Furthermore, a Late Permian to Early Triassic subduction is also well documented by contemporary deformation and high-pressure metamorphism in the Japanese islands ([Faure and Charvet, 1987] and [Faure et al., 1988]). However, in the central regions of the South China block, such as Jiangxi province, the Early Paleozoic structures are well preserved without obvious Early Mesozoic overprinting (Faure et al., 2009). Triassic granites are sparsely distributed in this region with crustal-derived signatures ([Gilder et al., 1996], [Zhou and Li, 2000] and [Zhou et al., 2006]). Thus, the far-field effect by the subduction is preferred than the flat-slab subduction. Accordingly, after a continuous deposition period from 400 Ma to 260 Ma, the South China block stepped out the stable period as evidenced by the onset of the Paleo-Pacific subduction around 260–250 Ma (e.g. Li et al., 2006). As the push force propagated to NW inland, the Chenzhou–Linwu fault as a weak zone, the Xuefengshan Belt commenced with NW verging folds and thrusts.

Analogous to other orogenic belts, such as the Alice Springs orogen, the Laramide orogen and the Pyrenees orogen ([Choukroune, 1992], [English and Johnston, 2004], [Hand and Sandiford, 1999] and [Sandiford et al., 2001]), a preexisting weak zone plays an important role in triggering an intracontinental orogeny. In the South China block, the Chenzhou–Linwu fault may represent such a weak zone. The Chenzhou–Linwu fault is interpreted as the Neoproterozoic suture zone between the Yangtze Block and the Cathaysia Block ([Wang et al., 2003] and [Yu et al., 2010]). Furthermore, this fault was active during the Neoproterozoic–Paleozoic rifting, and also during the development of the Early Paleozoic orogeny ([Faure et al., 2009] and [Wang and Li, 2003]). During the Early Mesozoic Xuefengshan orogeny, the Chenzhou–Linwu fault was easily reactivated in response to the far-field effect of the subduction at the southeastern continental margin of the South China block. And thereby the Xuefengshan intracontinental orogen is due to the reactivation at the Chenzhou–Linwu fault. The late-orogenic magmatism was generated in the last stage of the orogeny by crustal melting after the cessation of the compression.

6. Conclusion

Phanerozoic metaluminous to peraluminous granitoids are widespread in the Xuefengshan Belt. Combined with a synthesis of previous studies, geochronological and Lu—Hf isotopic data of representative plutons allow us to establish that:

(1)

The Early Paleozoic granites in the Xuefengshan Belt were emplaced during 430–410 Ma, with a time interval of ~ 20 Ma later than in the central part of the Wuyi–Baiyun–Yunkai orogen. The Xuefengshan Belt is partly involved in the Early Paleozoic deformation, but the recorded late-orogenic magmatism.

(2)

The Xuefengshan Belt is an Early Mesozoic orogen that experienced the late orogenic magmatism developed after the folding and the synmetamorphic ductile deformation. The emplacement of the Early Mesozoic plutons is well constrained during a rather short time span from 225 Ma to 215 Ma.

(3)

The Hf isotopic data of Early Mesozoic granites indicate a crustal-derived magma source without any input of mantle-derived materials. Hence, it is suggested that the Xuefengshan Belt is the tectonic result of the far-field effect of the Paleo-Pacific subduction from the southeastern margin of the South China block, but plutonism is not directly related with the flat-slab subduction.

Acknowledgments

Field works have been funded by the Innovative Project of the Chinese Academy of Sciences (Grant No. KZCX1-YW-15-1) and Major State Basic Research Development Program of China (2009CB825008). We thank Xin Yan and Saihong Yang for help with zircon CL imaging, Qiuli Li, Guoqiang Tang and Yu Liu for help with zircon U—Pb analysis, and Zhichao Liu and Yue-Heng Yang for help with zircon Hf analysis. Constructive reviews by Editor-in-Chief Nelson Eby, Guest Editor Prof. Xiaoyong Yang and two anonymous reviewers significantly improved the manuscript.

References

Brown, 2005 M. Brown Synergistic effects of melting and deformation: an example from the Variscan belt, western France ,in: D. Gapais, J.P. Brun, P. Cobbold (Eds.), Deformation Mechanisms, Rheology and Tectonics: From Minerals to the Lithosphere, Geological Society, London, Special Publication, 243 (2005), pp. 205–226

BGMRFJ, 1985 Bureau of Geology and Mineral Resources of Fujian Province (BGMRFJ) Regional Geology of the Jiangxi Province Geological Publishing House, Beijing (1985) 675 pp.

BGMRGX, 1985 Bureau of Geology and Mineral Resources of Guangxi province (BGMRGX) Regional Geology of the Guangxi Zhuang Autonomous Region Geological Publishing House, Beijing (1985) 853 pp.

BGMRGD, 1988 Bureau of Geology and Mineral Resources of Guangdong province (BGMRGD) Regional Geology of the Guangdong Province Geological Publishing House, Beijing (1988) 917 pp.

BGMRHN, 1988 Bureau of Geology and Mineral Resources of Hunan province (BGMRHN) Regional Geology of the Hunan Province Geological Publishing House, Beijing (1988) 507 pp.

BGMRJX, 1984 Bureau of Geology and Mineral Resources of Jiangxi Province (BGMRJX) Regional Geology of the Jiangxi Province Geological Publishing House, Beijing (1984) 921 pp.

BGMRZJ, 1989 Bureau of Geology and Mineral Resources of Zhejiang Province (BGMRZJ) Regional Geology of the Jiangxi Province Geological Publishing House, Beijing (1989) 617 pp.

Carter and Clift, 2008 Carter, P.D. Clift Was the Indosinian orogeny a Triassic mountain building or a thermotectonic reactivation event? Comptes Rendus Geosciences, 340 (2008), pp. 83–93

Carter et al., 2001 Carter, D. Roques, C. Bristow, P. Kinny Understanding Mesozoic accretion in Southeast Asia: significance of Triassic thermotectonism (Indosinian orogeny) in Vietnam Geology, 29 (2001), pp. 211–214

Charvet et al., 1996 J. Charvet, L.S. Shu, Y.S. Shi, L.Z. Guo, M. Faure The building of south China: Collision of Yangzi and Cathaysia blocks, problems and tentative answers Journal of Southeast Asian Earth Science, 13 (1996), pp. 223–235

Charvet et al., 2010 J. Charvet, L.S. Shu, M. Faure, F. Choulet, B. Wang, H.F. Lu, N. Le Breton

Structural development of the Lower Paleozoic belt of South China: genesis of an intracontinental orogeny Journal of Asian Earth Science, 39 (2010), pp. 309–330

Chen, 1999 Chen Mirror-image thrusting in the South China Orogenic Belt: tectonic evidence from western Fujian, southeastern China Tectonophysics, 305 (1999), pp. 497–519

Chen et al., 2006 W.F. Chen, P.R. Chen, X.M. Zhou, H.Y. Huang, X. Ding, T. Sun Single-zircon La-ICP-MS U—Pb dating of the Yangmingshan granitic pluton in Hunan, South China and its

petrogenetic study (in Chinese with English abstract) Acta Geologica Sinica, 80 (2006), pp. 1065–1077

Chen et al., 2007a W.F. Chen, P.R. Chen, H.Y. Huang, X. Ding, T. Sun Chronological and geochemical studies of granite and enclave in Baimashan pluton, Hunan, South China Science in China (D), 50 (2007), pp. 1606–1627

Chen et al., 2007b W.F. Chen, P.R. Chen, X.M. Zhou, H.Y. Huang, X. Ding, T. Sun Single Zircon LA-ICP-MS U—Pb dating of the Guandimiao and Wawutang granitic plutons in Hunan, South China and its petrogenetic significance Acta Geologica Sinica, 81 (2007), pp. 81–89

Choukroune, 1992 P. Choukroune Tectonic evolution of the Pyrenees Annual Review of Earth Planetary Sciences, 20 (1992), pp. 143–158

Chu et al., 2011 Y. Chu, M. Faure, W. Lin, Q. Wang Early Mesozoic intracontinental Xuefengshan Belt, South China: insights from structural analysis of polyphase deformation EGU meeting, Vienna, Austria (2011)

Chu et al., in press Chu, Y., Faure, M., Wang, Q.C., Ji, W.B., in press. Tectonics of the Middle Triassic intracontinental Xuefengshan Belt, South China: new insights from structural and chronological constraints on the basal décollement zone. International Journal of Earth Sciences.

Chung et al., 2005 S.L. Chung, M.F. Chu, Y. Zhang, Y. Xie, C.H. Lo, T.-Y. Lee, C.Y. Lan, X. Li, Q. Zhang, Y. Wang Tibetan tectonic evolution inferred from spatial and temporal variations in post-collisional magmatism Earth-Science Reviews, 68 (2005), pp. 173–196

Deprat, 1914 J. Deprat Etude des plissements et des zones décrasement de la moyenne et de la basse Rivière Noire Mémoire du Service Géologique Indochine, 3 (1914), p. 59

Ding et al., 2005 X. Ding, P.R. Chen, W.F. Chen, H.Y. Huang, X.M. Zhou LA-ICPMS zircon U—Pb age determination of the Weishan granite in Hunan: petrogenesis and significance Science in China (D), 35 (2005), pp. 606–616

English and Johnston, 2004 J.M. English, S.T. Johnston The Laramide orogeny: what were the driving forces? International Geology Review, 46 (2004), pp. 833–838

Faure and Charvet, 1987 M. Faure, J. Charvet Late Permian/early Triassic orogeny in Japan: piling up of nappes, transverse lineation and continental subduction of the Honshu block Earth and Planetary Science Letters, 84 (1987), pp. 295–308

Faure et al., 1988 M. Faure, P. Monié, O. Fabbri Microtectonics and ^{39}Ar–^{40}Ar dating of high pressure metamorphic rocks of the south Ryukyu Arc and their bearings on the pre-Eocene geodynamic evolution of Eastern Asia Tectonophysics, 156 (1988), pp. 133–143

Faure et al., 1996 M. Faure, Y. Sun, L. Shu, P. Monié, J. Charvet Extensional tectonics within a subduction-type orogen. The case study of the Wugongshan dome (Jiangxi Province, southeastern China) Tectonophysics, 263 (1996), pp. 77–106

Faure et al., 1999 M. Faure, W. Lin, L.S. Shu, Y. Sun, U. Scharer Tectonics of the Dabieshan (eastern China) and possible exhumation mechanism of ultra high-pressure rocks Terra Nova, 11 (1999), pp. 251–258

Faure et al., 2003 M. Faure, W. Lin, U. Scharer, L.S. Shu, Y. Sun, N. Arnaud Continental subduction and exhumation of UHP rocks. Structural and geochronological insights from the Dabieshan (East China) Lithos, 70 (2003), pp. 213–241

Faure et al., 2008 M. Faure, W. Lin, P. Monié, S. Meffre Paleozoic collision between the North and South China blocks, Early Triassic tectonics and the problem of the ultrahigh-pressure metamorphism Comptes Rendus Geosciences, 340 (2008), pp. 139–150

Faure et al., 2009 M. Faure, L.S. Shu, B. Wang, J. Charvet, F. Choulet, P. Monie Intracontinental subduction: a possible mechanism for the Early Palaeozoic Orogen of SE China Terra Nova, 21 (2009), pp. 360–368

Fromaget, 1932 J. Fromaget Sur la structure des Indosinides Comptes Rendus de l'Académie des Sciences, 195 (1932), p. 538

Gilder et al., 1996 S.A. Gilder, J. Gill, R.S. Coe, X.X. Zhao, Z.W. Liu, G.X. Wang, K.R. Yuan, W.L. Liu, G.D. Kuang, H.R. Wu Isotopic and paleomagnetic constraints on the Mesozoic tectonic evolution of south China Journal of Geophysical Research-Solid Earth, 101 (1996), pp. 16137–16154

Hacker and Wang, 1995 B.R. Hacker, Q.C. Wang Ar/Ar geochronology of ultrahigh-pressure metamorphism in Central China Tectonics, 14 (1995), pp. 994–1006

Hand and Sandiford, 1999 M. Hand, M. Sandiford Intraplate deformation in central Australia, the link between subsidence and fault reactivation Tectonophysics, 305 (1999), pp. 121–140

Harris and Massey, 1994 N. Harris, J. Massey Decompression and anatexis of Himalayan metapelites Tectonics, 13 (1994), pp. 1537–1546

Harrowfield and Wilson, 2005 M.J. Harrowfield, C.J.L. Wilson Indosinian deformation of the Songpan Garze Fold Belt, northeast Tibetan Plateau Journal of Structural Geology, 27 (1) (2005), pp. 101–117

Huang, 1960 T.K. Huang he main characteristics of the geologic structures of China: preliminary conclusions Acta Geologica Sinica, 40 (1960), pp. 1–37

Huang, 1978 T.K. Huang An outline of the tectonic characteristics of China Eclogae Geologicae Helvetiae, 71 (1978), pp. 611–635

Lepvrier et al., 1997 C. Lepvrier, H. Maluski, N. Van Vuong, D. Roques, V. Axente, C. Rangin Indosinian NW-trending shear zones within the Truong Son belt (Vietnam) ^{40}Ar–^{39}Ar Triassic ages and Cretaceous to Cenozoic overprints Tectonophysics, 283 (1997), pp. 105–127

Lepvrier et al., 2008 C. Lepvrier, N. Van Vuong, H. Maluski, P. Truong Thi, T. Van Vu Indosinian tectonics in Vietnam Comptes Rendus Geosciences, 340 (2008), pp. 94–111

Lepvrier et al., 2011 C. Lepvrier, M. Faure, V.N. Van, T.V. Vu, W. Lin, T.T. Trong, P.T. Hoa North-directed Triassic nappes in Northeastern Vietnam (East Bac Bo) Journal of Asian Earth Sciences, 41 (2011), pp. 56–68

Li, 1991 X.H. Li Geochronology of the Wanyangshan–Zhuguangshan granitoid batholith: implication for the crust development Science in China (B), 34 (1991), pp. 620–629

Li, 1994 X.H. Li A comprehensive U—Pb, Sm—Nd, Rb—Sr and ^{40}Ar–^{39}Ar geochronological study on Guidong Granodiorite, southeast China: records of multiple tectonothermal events in a single pluton Chemical Geology, 115 (1994), pp. 283–295

Li, 1998 Z.X. Li Tectonic history of the major East Asian lithospheric blocks since the mid-Proterozoic—a synthesis, in Flower, M.J., Chung, S.-L., Lo, C.-H., and Lee, T.-Y., eds., Mantle dynamics and plate inter actions in East Asia: Washington, D.C., American Geophysical Union Geodynamics Series, 27 (1998), pp. 221–243

Li, 1999 X.H. Li U—Pb zircon ages of granites from the southern margin of the Yangtze Block: timing of Neoproterozoic Jinning: orogeny in SE China and implications for Rodinia Assembly Precambrian Research, 97 (1999), pp. 43–57

Li and Li, 2007 Z.X. Li, X.H. Li Formation of the 1300-km-wide intracontinental orogen and postorogenic magmatic province in Mesozoic South China: a flat-slab subduction model Geology, 35 (2007), pp. 179–182

Li et al., 2002 Z.X. Li, X.H. Li, H.W. Zhou, P.D. Kinny Grenvillian continental collision in south China: new SHRIMP U—Pb zircon results and implications for the configuration of Rodinia Geology, 30 (2002), pp. 163–166

Li et al., 2006 X.H. Li, Z.X. Li, W.X. Li, Y.J. Wang Initiation of the Indosinian Orogeny in South China: evidence for a Permian magmatic arc on Hainan Island The Journal of Geology, 114 (2006), pp. 341–353

Li et al., 2008 H.Q. Li, D.H. Wang, F.W. Chen, Y.P. Mei, H. Cai Study on chronology of the Chanziping and Daping gold deposit in Xuefeng Mountains, Hunan Province Acta Geologica Sinica, 82 (2008), pp. 900–905 (in Chinese with English abstract)

Li et al., 2009a X.H. Li, W.X. Li, Z.X. Li, C.H. Lo, J. Wang, M.F. Ye, Y.H. Yang Amalgamation between the Yangtze and Cathaysia Blocks in South China: constraints from SHRIMP U—Pb zircon ages, geochemistry and Nd—Hf isotopes of the Shuangxiwu volcanic rocks Precambrian Research, 174 (2009), pp. 117–128

Li et al., 2009b X.H. Li, Y. Liu, Q.L. Li, C.H. Guo, K.R. Chamberlain Precise determination of Phanerozoic zircon Pb/Pb age by multicollector SIMS without external standardization

Geochemistry Geophysics Geosystems, 10 (2009), p. Q04010
http://dx.doi.org/10.1029/2009GC002400

Li et al., 2010a Q.L. Li, X.H. Li, Y. Liu, G.Q. Tang, J.H. Yang, W.G. Zhu Precise U—Pb and Pb—Pb dating of Phanerozoic baddeleyite by SIMS with oxygen flooding technique Journal of Analytical Atomic Spectrometry, 25 (2010), pp. 1107–1113

Li et al., 2010b Z.X. Li, X.H. Li, J.A. Wartho, C. Clark, W.-X. Li, C.L. Zhang, C. Bao Magmatic and metamorphic events during the early Paleozoic Wuyi–Yunkai orogeny, southeastern South China: new age constraints and pressure–temperature conditions Geological Society of America Bulletin, 122 (2010), pp. 772–793

Li et al., 2011 L.M. Li, M. Sun, Y. Wang, G. Xing, G. Zhao, S. Lin, X. Xia, L. Chan, F. Zhang, J. Wong U—Pb and Hf isotopic study of zircons from migmatised amphibolites in the Cathaysia Block: implications for the early Paleozoic peak tectonothermal event in Southeastern China Gondwana Research, 19 (2011), pp. 191–201

Lin et al., 2000 W. Lin, M. Faure, P. Monie, U. Scharer, L.S. Zhang, Y. Sun Tectonics of SE China: new insights from the Lushan massif (Jiangxi Province) ectonics, 19 (2000), pp. 852–871

Lin et al., 2008 W. Lin, Q.C. Wang, K. Chen Phanerozoic tectonics of south China block: new insights from the polyphase deformation in the Yunkai massif Tectonics, 27 (2008), p. TC6004 http://dx.doi.org/10.1029/2007TC002207

Ludwig, 2001 K.R. Ludwig Users manual for Isoplot/Ex rev. 2.49 Berkeley Geochronology Centre Special Publication, No. 1a (2001) 56 pp.

Morel et al., 2008 M.L.A. Morel, O. Nebel, Y.J. Nebel-Jacobsen, J.S. Miller, P.Z. Vroon Hafnium isotope characterization of the GJ-1 zircon reference material by solution and laser-ablation MC-ICPMS Chemical Geology, 255 (2008), pp. 231–235

Qiu et al., 1999 Y.X. Qiu, Y.C. Zhang, W.P. Ma The Tectonic Nature and Evolution of Xuefeng Mountains: One Model of Formation and Evolution of Intra-continental Orogenic Belt Geological Publishing House, Beijing (1999) 155 pp.

Qiu et al., 2000 Y.M. Qiu, S. Gao, N.J. McNaughton, D.I. Groves, W. Ling First evidence of > 3.2 Ga continental crust in the Yangtze craton of south China and its implications for Archean crustal evolution and Phanerozoic tectonics Geology, 28 (2000), pp. 11–14

Ren, 1991 J. Ren On the geotectonics of southern China Acta Geologica Sinica, 44 (1991), pp. 111–130

Roger et al., 2004 F. Roger, J. Malavieille, P.H. Leloup, S. Calassou, Z. Xu Timing of granite emplacement and cooling in the Songpan-GarzeFold Belt (eastern Tibetan Plateau) with tectonic implications Journal of Asian Earth Sciences, 22 (2004), pp. 465–481

Roger et al., 2010 F. Roger, M. Jolivet, J. Malavieille The tectonic evolution of the Songpan-Garze (North Tibet) and adjacent areas from Proterozoic to Present: a synthesis Journal of Asian Earth Sciences, 39 (2010), pp. 254–269

Sandiford et al., 2001 M. Sandiford, M. Hand, S. McLaren Tectonic Feedback, Intraplate Orogeny and the Geochemical Structure of the Crust: A Central Australian Perspective Geological Society, London, Special Publications, 184 (2001), pp. 195–218

Shu et al., 1994 L.S. Shu, G.Q. Zhou, Y.S. Shi, J. Yin Study of the high-pressure metamorphic blueschist and its Late Proterozoic age in the Eastern Jiangnan Belt Chinese Science Bulletin, 39 (1994), pp. 1200–1204

Shu et al., 2009 L.S. Shu, X.M. Zhou, P. Deng, B. Wang, S.Y. Jiang, J.H. Yu, X.X. Zhao Mesozoic tectonic evolution of the Southeast China Block: new insights from basin analysis Journal of Asian Earth Sciences, 34 (2009), pp. 376–391

Sláma et al., 2008 J. Sláma, J. Košler, D.J. Condon, J.L. Crowley, A. Gerdes, J.M. Hanchar, M.S.A. Horstwood, G.A. Morris, L. Nasdala, N. Norberg, U. Schaltegger, B. Schoene, M.N. Tubrett, M.J. Whitehouse Plešovice zircon—a new natural reference material for U—Pb and Hf isotopic microanalysis Chemical Geology, 249 (2008), pp. 1–35

Stacey and Kramers, 1975 J.S. Stacey, J.D. Kramers pproximation of terrestrial lead isotope evolution by a two-stage model Earth Planetary Science Letters, 26 (1975), pp. 207–221

Wan et al., 2010 Y. Wan, D. Liu, S.A. Wilde, J. Cao, B. Chen, C. Dong, B. Song, L. Du Evolution of the Yunkai Terrane, South China: evidence from SHRIMP zircon U—Pb dating, geochemistry and Nd isotope Journal of Asian Earth Sciences, 37 (2010), pp. 140–153

Wang and Li, 2003 J. Wang, Z.X. Li History of Neoproterozoic rift basins in South China: implications for Rodinia break-up Precambrian Research, 122 (2003), pp. 141–158

Wang et al., 2003 Y.J. Wang, W.M. Fan, F. Guo, T.P. Peng, C.W. Li Geochemistry of Mesozoic mafic rocks adjacent to the Chenzhou-Linwu fault, South China: implications for the lithospheric boundary between the Yangtze and Cathaysia blocks International Geology Review, 45 (2003), pp. 263–286

Wang et al., 2005 Y.J. Wang, Y.H. Zhang, W.M. Fan, T.P. Peng Structural signatures and Ar-40/Ar-39 geochronology of the Indosinian Xuefengshan tectonic belt, South China Block Journal of Structural Geology, 27 (2005), pp. 985–998

Wang et al., 2007a Y.J. Wang, W.M. Fan, M. Sun, X.Q. Liang, Y.H. Zhang, T.P. Peng Geochronological, geochemical and geothermal constraints on petrogenesis of the Indosinian peraluminous granites in the South China Block: a case study in the Hunan Province Lithos, 96 (2007), pp. 475–502

Wang et al., 2007b Y.J. Wang, W.M. Fan, G.C. Zhao, S.C. Ji, T.P. Peng Zircon U—Pb geochronology of gneissic rocks in the Yunkai massif and its implications on the Caledonian event in the South China Block Gondwana Research, 12 (2007), pp. 404–416

Woodhead and Hergt, 2005 J.D. Woodhead, J.M. Hergt A preliminary appraisal of seven natural zircon reference materials for in situ Hf isotope determination Geostandards and Geoanalytical Research, 29 (2005), pp. 183–195

Wu et al., 2006 F.Y. Wu, Y.H. Yang, L.W. Xie, J.H. Yang, P. Xu Hf isotopic compositions of the standard zircons and baddeleyites used in U—Pb geochronology Chemical Geology, 234 (2006), pp. 105–126

Xu et al., 2004 H.J. Xu, C.Q. Ma, Y.F. Zhong, Z.B. She Zircon SHRIMP dating of Taojiang and Dashenshan granite: lower limit on the timing of the amalgamation between Yangtze and Cathaysia blocks Annual meeting of Petrology and Geodynamics, China (2004)

Xu et al., 2005 X.S. Xu, S.Y. O'Reilly, W.L. Griffin, P. Deng, N.J. Pearson Relict proterozoic basement in the Nanling Mountains (SE China) and its tectonothermal overprinting Tectonics, 24 (2005) http://dx.doi.org/10.1029/2004TC001652

Xu et al., 2011 X.B. Xu, Y.Q. Zhang, L.S. Shu, D. Jia La-ICP-MS U—Pb and $^{40}Ar/^{39}Ar$ geochronology of the sheared metamorphic rocks in the Wuyishan: Constraints on the timing of Early Paleozoic and Early Mesozoic tectono-thermal events in SE China Tectonophysics, 501 (2011), pp. 71–86

Yan et al., 2003 D.P. Yan, M.F. Zhou, H.L. Song, X.W. Wang, J. Malpas Origin and tectonic significance of a Mesozoic multi-layer over-thrust system within the Yangtze Block (South China) Tectonophysics, 361 (2003), pp. 239–254

Yan et al., 2006 D.P. Yan, M.F. Zhou, C.Y. Wang, B. Xia Structural and geochronological constraints on the tectonic evolution of the Dulong-Song Chay tectonic dome in Yunnan Province, SW China Journal of Asian Earth Sciences, 28 (2006), pp. 332–353

Yang et al., 2010 D.S. Yang, X.H. Li, W.X. Li, X.Q. Liang, W.G. Long, X.L. Xiong U—Pb and ^{40}Ar—^{39}Ar geochronology of the Baiyunshan gneiss (central Guangdong, south China): constraints on the timing of early Palaeozoic and Mesozoic tectonothermal events in the Wuyun (Wuyi–Yunkai) Orogen Geological Magazine, 147 (2010), pp. 481–496

Yu et al., 2009 J.-H. Yu, L. Wang, S.Y. O'Reilly, W.L. Griffin, M. Zhang, C. Li, L. Shu A Paleoproterozoic orogeny recorded in a long-lived cratonic remnant (Wuyishan terrane), eastern Cathaysia Block, China Precambrian Research, 174 (2009), pp. 347–363

Yu et al., 2010 J.H. Yu, S.Y. O'Reilly, L. Wang, W.L. Griffin, M.-F. Zhou, M. Zhang, L. Shu Components and episodic growth of Precambrian crust in the Cathaysia Block, South China: evidence from U—Pb ages and Hf isotopes of zircons in Neoproterozoic sediments Precambrian Research, 181 (2010), pp. 97–114

Zhang et al., 2006a S.B. Zhang, Y.-F. Zheng, Y.-B. Wu, Z.-F. Zhao, S. Gao, F.-Y. Wu Zircon U—Pb age and Hf isotope evidence for 3.8 Ga crustal remnant and episodic reworking of Archean crust in South China Earth and Planetary Science Letters, 252 (2006), pp. 56–71

Zhang et al., 2006b S.-B. Zhang, Y.-F. Zheng, Y.-B. Wu, Z.-F. Zhao, S. Gao, F.-Y. Wu Zircon isotope evidence for ≥ 3.5 Ga continental crust in the Yangtze craton of China Precambrian Research, 146 (2006), pp. 16–34

Zhang et al., 2011 F. Zhang, Y. Wang, X. Chen, W. Fan, Y. Zhang, G. Zhang, A. Zhang Triassic high-strain shear zones in Hainan Island (South China) and their implications on the amalgamation of the Indochina and South China Blocks: kinematic and $^{40}Ar/^{39}Ar$ geochronological constraints Gondwana Research, 19 (2011), pp. 910–925

Zheng et al., 2004 J.P. Zheng, W.L. Griffin, S.Y. O'Reilly, M. Zhang, N. Pearson, Y. Pan Widespread Archean basement beneath the Yangtze craton Geology, 34 (2004), pp. 417–420

Zheng et al., 2010 J.P. Zheng, W.L. Griffin, L.S. Li, S.Y. O'Reilly, N.J. Pearson, H.Y. Tang, G.L. Liu, J.H. Zhao, C.M. Yu, Y.P. Su Highly evolved Archean basement beneath the western Cathaysia Block, South China Geochemica et Cosmochimica Acta, 75 (2010), pp. 242–255

Zhou, 2007 X.M. Zhou (Ed.), Genesis of Late Mesozoic Granites in Nanling Region and Geodynamic Evolution of Lithosphere, Science Press, Beijing (2007) 691 pp.

Zhou and Li, 2000 X.M. Zhou, W.X. Li Origin of Late Mesozoic igneous rocks in Southeastern China: implications for lithosphere subduction and underplating of mafic magmas Tectonophysics, 326 (2000), pp. 269–287

Zhou et al., 2006 X.M. Zhou, T. Sun, W.Z. Shen, L.S. Shu, Y.L. Niu Petrogenesis of Mesozoic granitoids and volcanic rocks in South China: a response to tectonic evolution Episodes, 29 (2006), pp. 26–33